Long-acting genipin derivative protects retinal ganglion cells from oxidative stress models in vitro and in vivo through the Nrf2/antioxidant response element signaling pathway

著者	Koriyama Yoshiki, Chiba Kenzo, Yamazaki Matsumi, Suzuki Hirokazu, Muramoto Ken-ichiro, Kato Satoru
journal or publication title	Journal of Neurochemistry
volume	115
number	1
page range	79-91
year	2010-10-01
URL	http://hdl.handle.net/2297/25490

doi: 10.1111/j.1471-4159.2010.06903.x

Long-acting genipin derivative protects retinal ganglion cells from oxidative stress models *in vitro* and *in vivo* through the Nrf2/antioxidant response element signaling pathway.

Yoshiki Koriyama*[1, 4], Kenzo Chiba[2, 4], Matsumi Yamazaki[2], Hirokazu Suzuki[3, 4], Ken-ichiro Muramoto[5] and Satoru Kato[1]

[1]Department of Molecular Neurobiology, Graduate School of Medicine, Kanazawa University, 13-1 Takaramachi, Kanazawa 920-8640, Japan

[2]Department of Biochemistry and [3]Department of Medicinal Chemistry, Faculty of Pharmaceutical Sciences, Hokuriku University,

[4]Organization for Frontier Research in Preventive Pharmaceutical Sciences, Hokuriku University, Ho-3 Kanagawa-machi, Kanazawa, Ishikawa 920-1181, Japan,

[5]Information Engineering, Graduate School of Natural Science, Kanazawa University, Kakuma-machi, Kanazawa, Ishikawa, 920-1192, Japan

Keywords: Nitric oxide, S-nitrosylation, Keap1, retinal ganglion cell, oxidative stress, HO-1

Running title: genipin prevents apoptosis via Nrf2/ARE system

Abbreviations:

ARE, antioxidant response element;

ChIP, Chromatin immunoprecipitation;

c-PTIO, 2-(4-carboxyphenyl)-4,4,5,5-tetramethylimidazoline-1-oxyl-3-oxide;

DAF-2DA; Diaminofluorescein–2 Diacetate;

GCL, ganglion cell layer;

GCLC, glutamate cysteine ligase catalytic subunit;

4HNE, 4-hydroxy-2-nonenal;

HO, heme oxygenase;

IPRG001, (1R)-*iso*Propyloxygenipin;

Keap1, Kelch-like ECH-associated protein;

LY, LY294002;

MTT, 3-[4, 5-dimethylthiazol-2-yl]-2,5-diphenyltetrazolium bromide;

NO, nitric oxide;

NOS, nitric oxide synthase;

NQO-1, NAD(P)H: quinine oxidoreductase-1;

Nrf2, NF-E2-related factor 2;

ONI, optic nerve injury;

PI3K, phosphatidylinositol 3-kinase;

RGC, retinal ganglion cell;

SnMP, Sn-mesoporphyrin;

WT, wortmannin;

*Address for correspondence: Department of Molecular Neurobiology, Graduate School of Medicine, Kanazawa University, Kanazawa 920-8640, Japan

TEL: 81 76 265 2451

FAX: 81 76 234 4235

E-mail: koriyama@med.kanazawa-u.ac.jp

Abstract

Previously, we reported that genipin, a herbal iridoid, had neuritogenic and neuroprotective actions on PC12 cells. Although nitric oxide (NO)-activated signalings were proposed to be neuritogenic, the neuroprotective action of genipin remains to be elucidated. From the standpoint of NO-activation, we tested a possible protective mechanism through the nitrosative Keap1/Nrf2-antioxidant response element (ARE) pathway in rat retinal ganglion cells (RGC-5 cells) in culture, and *in vivo*, against hydrogen peroxide and optic nerve injury (ONI) respectively, using a long-acting (1R)-isoPropyloxygenipin (IPRG001). IPRG001 induced NO generation and the expressions of antioxidative enzymes, such as heme oxygenase-1 (HO-1), in RGC-5 cells. The protective action of IPRG001 depended on HO-1 and NO induction. We found that S-nitrosylation of Keap1 by IPRG001 may contribute to translocation of Nrf2 to the nucleus and triggered transcriptional activation of antioxidative enzymes. Furthermore, apoptotic cells were increased and 4-hydroxy-2-nonenal (4HNE) was accumulated in rat retina following ONI. Pretreatment with IPRG001 almost completely suppressed apoptosis and accumulation of 4HNE in RGCs following ONI accompanied by HO-1 induction. These data demonstrate for the first time that IPRG001 exerts neuroprotective action in RGCs in vitro and in vivo, through the Nrf2/ARE pathway by S-nitrosylation against oxidative stress.

Introduction

We previously reported that a plant-derived iridoid compound, genipin, had neurotrophic - neuritogenic and neuroprotective - action on neural cell lines, PC12h cells (Yamazaki *et al*. 1996, 2001a, 2004) and Neuro2a cells (Yamazaki and Chiba, 2005, Yamazaki *et al*., 2008). We proposed that the nitric oxide (NO)-activated protein kinase system was involved with the neuritogenesis of genipin. NO donor and cGMP produced a promotion of neurite outgrowth from PC12h cells, whereas nitric oxide synthetase inhibitor, NO-scavenger and cGMP-dependent protein kinase (PKG) inhibitor all abolished its action (Yamazaki *et al*. 2001a, 2004). These results strongly indicate that the neurite outgrowing action of genipin works with NO-cGMP-PKG signaling.

In contrast to the neuritogenic action, the neuroprotective action of genipin remained to be elucidated. It also remained to be determined whether the neurotrophic effects of genipin are confined to neuronal cell lines in culture, or extend to nervous tissues *in vivo*. The objective of this study was to answer the two questions: (1) What is the neuroprotective mechanism of genipin? (2) Does genipin exert neuroprotective action on nervous tissues *in vivo*?

Genipin protected neurotoxicity induced by 6-hydroxydopamine, β-amyloid protein and serum free conditions (Yamazaki *et al*. 2001b, 2008, Yamazaki and Chiba, 2005). The toxicity that underpins these insults was partly ascribed to the generation of reactive oxygen species (ROS). Recently, we investigated the protective action of 5-S-GAD, a radical scavenging peptide on rat retinal ganglion-like cell line (RGC-5 cells), and rat retinal ganglion cells (RGCs) with *in vitro* and *in vivo* models against various cytotoxic (hydrogen peroxide (H_2O_2), NMDA, serum free condition and optic nerve injury(ONI)) insults (Koriyama *et al*. 2008, 2009b). These toxic insults also generate ROS. Before

starting the experiments, we chemically synthesized an alkylating genipin, which is a stable and long-acting derivative for *in vivo* studies (Suzuki *et al*. 2010). We used a genipin derivative, (1R)-*iso*Propyloxygenipin (IPRG001), throughout this *in vitro* and *in vivo* study.

As for the neuroprotective action, we focused on the NO activation mechanism against various oxidative stress mentioned above. It is well known that antioxidative proteins play a key role in the protective action against oxidative stress. Such antioxidative proteins including heme oxygenase-1 (HO-1: EC 1.14.99.3) are induced by activation of Keap1/Nrf2-antioxidative response element (ARE) signaling (Kaspar *et al*., 2009, Kurauchi *et al*., 2009). In the present study, we investigated a possible neuroprotective mechanism of IPRG001 through the Nrf2/ARE pathway in the cultured RGC-5 cells, and rat RGCs against H_2O_2 and ONI, respectively.

Genipin is a putative therapeutic tool for preventing cell death against various neurodegenerative diseases, such as glaucoma.

Materials and methods

Chemicals

A long-acting genipin derivative (IPRG001) was synthesized as previously reported (Suzuki *et al*., 2010). Original genipin was purchased from Wako Pure Chemical Industries, Ltd. (Osaka, Japan). Genipin and IPRG001 were dissolved in dimethyl sulfoxide. 2-(4-Carboxyphenyl)-4, 4, 5, 5-tetramethylimidazoline-1-oxyl-3-oxide, sodium salt (c-PTIO), (±)-(E)-4-Methyl-2-[(E)-hydroxyimino]-5-nitro-6-methoxy-3-hexenamide (NOR-1), a NO donor and 4', 6-diamino-2-phenylindole (DAPI) were obtained from Dojindo (Japan). The phosphatidylinositol 3-kinase (PI3K) inhibitors, wortmannin (WT) and LY294002 (LY) were purchased from Sigma-Aldrich (ST Louis, MO, USA). An HO-1 inhibitor, Sn-mesoporphyrin (SnMP), was obtained from Frontier Scientific Inc. (Logan, UT).

Cell culture

RGC-5 cells were kindly provided by Dr. N. Agarwal, University of North Texas Health Science Center and Dr. H. Hara, Gifu Pharmaceutical University. RGC-5 cells were cultured in low-glucose Dulbecco's modified Eagle's medium (DMEM), containing 10% fetal calf serum (FBS), 100 U/ml of penicillin and 100 μg/ml of streptomycin in a humidified atmosphere of 95% air and 5% CO_2 at 37°C. The cells were passaged by trypsinization every 3-4 days. RGC-5 cells (5×10^3 cells/ml) were cultured overnight before use. After washing with DMEM, the cells were cultured in medium containing 1% FBS to avoid over cell growth.

Measurement of NO production

The fluorescent dye, 4, 5-diaminofluorescein diacetate (DAF-2DA; Daiichi Pure Chemicals, Tokyo) is an indicator of NO production. RGC-5 cells were cultured and washed twice with Earle's balanced salt solution (EBSS), treated with IPRG001 at 37°C for 1 h, and then to which DAF-2DA at 10 μM was added to the culture dishes each time (30 min-2 h). The samples were then washed with EBSS and centrifuged at 100 g for 5 min at room temperature. The supernatants were discarded, and 500 μl of EBSS was added to each cell pellet. The fluorescence intensity of each cell suspension was measured by the emission at a wavelength of 515 nm, and excitation wavelength of 495 nm using a Fluoroskan Ascent plate reader (Thermo Lab system).

MTT assay

Cell death was estimated using a 3-(4, 5-dimethylthiazol-2-yl)-2, 5-diphenyltetrazolium bromide (MTT) assay. An aliquot (20 μl) of 2.75 mg/ml MTT in phosphate-buffered saline (PBS) was added to 200 μl of each culture medium as described previously (Koriyama *et al*. 2003). The reaction mixtures were incubated at 37°C for 3 h, prior to adding 200 μl HCl/isopropanol. The resultant formazan was measured by its absorbance at 550 nm using a plate reader (Model 680, Bio-Rad Laboratories, Hercules, CA). The experiments were repeated at least three times and compared with the control experiment.

RNA isolation and RT-PCR

Total RNA was isolated from RGC-5 cells using Sepasol RNAI (Nacalai Tesque, Japan). Four types of cDNA fragments were obtained by RT-PCR, using an RNA PCR kit (AMV) Ver.3 (TaKaRa, Japan) with following specific primers. To HO-1: 5′-AGCATGTCCCAGGATTTGTC -3′(forward) and

5′-ACCAGCAGCTCAGGATGAGT-3′ (reverse), heme oxigenase-2 (HO-2): 5′-GAAGGAAGGGACCAAGGAAG -3′ (forward) and 5′-GAGTTTTAGTGCCCGCTGAG -3′ (reverse), Nrf2: 5′-CAGTCTTCACCACCCCTGAT -3′ (forward) and 5′-CTAATGGCAGCAGAGGAAGG-3′ (reverse), NAD(P)H: quinine oxidoreductase-1 (NQO-1): 5′-GCCCGGATATTGTAGCTGAA-3′ (forward), 5′-AAGACCTGGAAGCCACAGAA-3′ (reverse), and glutamate cysteine ligase catalytic subunit (GCLC): 5′-TCAAAGGCCTCTAAGCCAGA-3′ (forward), 5′-AGATCTCCGTGTCGATGGTC-3′ (reverse). The products of PCR were electrophoresed and stained with ethidium bromide. The product bands were quantified using Scion Image software (Scion Corporation, USA), and normalized by the corrected data of glyceraldehyde-3-phosphate dehydrogenase (GAPDH) mRNA.

S-Nitrosylation analyses of Keap1

S-Nitrosylation of Keap1 was assessed by a modified biotin switch assay (Jaffrey et al. 2001) using the S-nitrosylated Protein Detection Assay Kit (Cayman Chemical). RGC-5 cells exposed to 50 μM NOR1 or 20 μM IPRG001 for 1 h were harvested and lysed at 4°C. Free thiols were blocked by adding S-methyl methanethiosulfonate. Biotinylation of nitrosothiols was carried out by maleimide-biotin. Biotinylated proteins were further purified by overnight incubation with neutravidin-coupled agarose beads (Pierce-Thermo Scientific). After incubation, beads were washed three times with PBS. Isolated proteins were recovered from beads by addition of Laemmli sample buffer, and heated at 85°C for 10 min. The amount of S-nitrosylated Keap1 protein in the samples was analyzed by western blot analysis using anti-Keap1 antibody (Santa Cruz Biotechnology, CA, USA).

Subcellular fractions of Nrf2 protein

Cells were lysed by hypotonic lysis buffer containing 10 mM HEPES-KOH (pH7.9), 10 mM KCl, 1.5 mM $MgCl_2$, 1 mM DTT, 0.5 mM phenylmethylsulfonyl fluoride, proteases inhibitor cocktail and centrifuged at 10,000 rpm for 15 min at 4°C. The supernatants were used as a cytoplasmic fraction. The pellets were incubated with a nuclear lysis buffer containing 20 mM HEPES-KOH (pH7.9), 400 mM NaCl, 1.5 mM $MgCl_2$, 0.2 mM EDTA, 1 mM DTT, 5% glycerol, protease inhibitor cocktail (Sigma) and further incubated for 30 min on ice. The lysates were centrifuged at 13,000 rpm for 15 min at 4°C. The supernatants were used as nuclear fraction samples. Immunoblotting analysis of β-actin and histon H4 was performed to ensure no contamination between cytoplasmic and nuclear fractions.

Western blot analysis

RGC-5 cells cultured under various conditions were extracted and their aliquots (30 μg of protein) were subjected to polyacrylamide gel electrophoresis using a 12.5% gel as described previously (Koriyama *et al*. 2009a). The separated proteins were transferred to a nitrocellulose membrane and incubated with primary and secondary antibodies (purchased from Santa Cruz Biotechnology, CA, USA). The signals for the antibody-bound protein bands (57 kDa for Nrf2; 68 kDa for Keap1) were detected using BCIP/NBT Kit (KPL, Gaithersburg, MD). An antibody against β-actin was used as an internal standard. The protein bands isolated in samples from cells under various culture conditions were analyzed densitometrically using the Scion Image Software (Scion Corp.). All experiments were repeated at least three times.

siRNA for HO-1 gene

We used small interfering RNA (siRNA) for the target region to rat HO-1 mRNA, 5'-GGAAUUUAUGCCAUUAAAUG-3' (sense), 5'-UUUACAUGGCAUAAAUUCCCA-3' (antisense), (Sigma-Aldrich, Tokyo, Japan) and randomly shuffled sequence 5'-GGUUGAUUAACGUAUUCGAAG -3' (sense), 5'-UAGAAUACGUUAAUCAACCCU -3' (antisense). Transfection of siRNA into the RGC-5 cell was carried out using Lipofectamine 2000 (Invitrogen Corporation, Carlsbad, CA, USA). To suppress HO-1 expression at the transcription levels, RGC-5 cells were incubated for 24 h with siRNA (100 pmol).

Chromatin immunoprecipitation (ChIP) assay

ChIP assays were performed by ChIP Assay Kit (Upstate/Millipore Corporation, Temecula, CA, USA). Briefly, proteins and DNA were cross-linked with formaldehyde and cells were lysed in SDS-lysis buffer and then sonicated. To reduce non-specific background, the sheared chromatin was incubated with Protein A agarose/ Salmon Sperm DNA. The remaining chromatin was immunoprecipitated with IgG (as control) or Nrf2 antibodies. DNA-protein complexes were eluted from the antibody with elution buffer containing 1% SDS and 0.1 M $NaHCO_3$, as well as formaldehyde reversed cross-links by 5 M of NaCl and heating at 65°C for 4 h. DNA was purified and PCR was performed using primers that spanned the rat HO-1 E1 enhancer (Alam and Cook, 2003). The primers used were: E1, 5′- GATTTCCTCACTGCCCTGAA -3′ (forward) and 5′- CTTCTGCCCGAGGTTAAAGC -3′ (reverse). A 1.5% agarose gel with ethidium bromide was used to separate and examine the PCR products.

Animals and Surgery

Sprague–Dawley rats (body-weight 250-300 g) were used. Rats were reared and handled according to the NIH guidelines and ARVO statement on the care and use of laboratory animals. Rats were anesthetized by intraperitoneal injection of sodium pentobarbital (30-40 mg/kg body weight). Intravitreal injection was performed with a Hamilton microsyringe 30G needle. The volume of injection was set at 5 μl of total volume after pre-suction of the same volume of vitreal fluid. One day after applying IPRG001 with or without SnMP, the optic nerve was crushed 1mm away from the eyeball with forceps as described previously (Koriyama *et al*. 2008). Rats were reared in clear plastic cages and kept under 12h/12h light dark cycle at 23°C.

Immunohistochemistry

Tissue fixation and cryosection were performed as described previously (Koriyama *et al*. 2009b). Briefly, the eyes were enucleated and fixed in 4% paraformaldehyde solution containing 0.1 M phosphate buffer (pH 7.4), and 5% sucrose for 2 h at 4°C. Sucrose concentration was gradually increased from 5 to 20%. The eyes were then embedded in optimal cutting temperature (OCT) compound (Tissue Tek; Miles, Eikhart, IN) and cryosectioned at 12 μm thickness. The frozen sections were mounted onto silane-coated glass slides and air-dried. After washing and blocking with Blocking One (Nakalai Tesque, Kyoto), retinal sections were incubated with the primary anti-HO-1 antibody (Santa Cruz Biotechnology, 1:300) and TUJ-1 (R&D systems, Minneapolis, USA) at 4°C overnight. The sections were then incubated with Alexafluoro anti-IgG (Molecular probe, 1:2000) at room temperature. In the Nrf2 translocation study, RGC-5 cells were fixed by 0.1% glutaraldehyde (Wako, Osaka, Japan) for 30 min at room temperature. Nrf2 translocation to the nucleus was stained using anti-Nrf2 antibody and

4',6-diamino-2-phenylindole (DAPI) nuclei staining dye.

Terminal transferase dUTP nick-end labeling (TUNEL) staining

After fixation and cryosection, retinal sections were incubated in 0.1% Triton X-100, as well as 0.1% sodium citrate for 15 min and rinsed in PBS. DNA fragmentation of cells undergoing apoptosis was detected using an *in situ* cell death detection kit (Roche, Mannheim, Germany), containing terminal transferase and fluorescence dUTP. The retinal sections were incubated in this reaction mixture overnight at 37˚C, and rinsed twice in PBS. In each retina, the number of TUNEL-positive cells within 300 μm from the optic disc was counted.

Dot blotting analysis for 4-hydroxy-2-nonenal (4HNE)

To assess the antioxidant effect of IPRG001, we performed dot blotting analysis for the 4HNE, a marker of lipid peroxidation. After 1 day of pretreatment with IPRG001, with or without SnMP and 4 days of treatment with ONI, the retinal samples were isolated and homogenized. Equal amounts of protein (30 μg) were applied to a Hybri-SLOT apparatus (Gibco BRL) and transferred to a nitrocellulose membrane (Whatman) by vacuum filtration. After blocking with 3% BSA for 1 h at room temperature, the samples were incubated with an anti-4HNE antibody (1:100; NOF Corporation) at 4°C overnight, followed by incubation with anti-mouse IgG antibody (Santa Cruz Biotechnology, CA, USA) for 1 h at room temperature. Antibody-bound protein bands were detected using BCIP/NBT Kit and analyzed densitometrically as described above. All experiments were repeated at least three times.

Statistics

All results are reported as means ± S.E.M for 3-5 experiments. Differences between groups were analyzed using ANOVA, followed by Dunnett's multi-comparison test with PASW Software (SPSS Inc., USA). P-values < 0.05 were considered statistically significant.

Results

Nitric oxide (NO) generation by IPRG001 ←----Fig. 1

First, we tested NO-inducibility of IPRG001, because of its leading molecule as the first step of our neuroprotective hypothesis for genipin. 20 μM of IPRG001 significantly increased the fluorescence intensity of DAF-2DA, a trapping indicator of NO in RGC-5 cells 0.5-2 h after IPRG001 treatment (Figure 1A). The increased intensity was 1.4-fold at 0.5 h, 1.5-fold at 1 h, 1.7-fold at 2 h and 1.8-fold at 4 h (data not shown) after treatment. Intensive green fluorescent cells could be seen in the RGC-5 cells in culture within 1 h of incubation with IPRG001 (Figure 1D) as compared to no treatment (Figure 1B). Figures 1C and 1E showed counterstaining of RGC-5 cell nuclei with DAPI.

Protective effect of IPRG001 and NO related compounds in the RGC-5 cells against H_2O_2 exposure. ←----Fig. 2

To evaluate the neuroprotective effect of IPRG001 in RGC-5 cells against oxidative stress, we constructed a cytotoxic model of hydrogen peroxide (H_2O_2) exposure in culture. 300 μM of H_2O_2 induced cell death in 60% of total RGC-5 cells for 24 h (Figure 2A). IPRG001 at 5-20 μM dose-dependently suppressed cell death induced by H_2O_2. 20 μM of IPRG001 rescued 85% of total RGC-5 cells under H_2O_2 exposure

(Figure 2A). IPRG001 alone did not produce any change in cell viability (Figure 2A). In these experiments, IPRG001 was added to the culture medium 4 h before H_2O_2 exposure, because NO production by IPRG001 was maximized within 4 h following incubation (Figure 1). In Figure 2B, we decided the pretreatment time with IPRG001 before H_2O_2 exposure. The maximum protective effect could be seen at 4-6 h of IPRG001 pretreatment before H_2O_2 addition, but no protective effect could be seen at 0-2 h of pretreatment with IPRG001 before H_2O_2 exposure (Figure 2B). NOR1, a NO donor also protected RGC-5 cell death following H_2O_2 exposure (Figure 2C). 50 μM of NOR1 was almost equivalent to 20 μM of IPRG001 in the neuroprotection against H_2O_2 (Figure 2C). NOR1 alone did not affect cell viability in any concentrations. On the other hand, c-PTIO, a NO scavenger completely suppressed the protective effect of IPRG001 (Figure 2D). This neuroprotective effect of IPRG001 on RGC-5 cells against H_2O_2 exposure was also completely suppressed by 20 μM cycloheximide (CHX), a protein synthesis inhibitor (Figure 2D). No effect could be seen in c-PTIO or CHX alone (Figure 2D).

IPRG001 induces antioxidative proteins in RGC-5 cells. **←----Fig. 3**

As the protective effect of IPRG001 was dependent upon newly synthesized protein(s), we next tested the inducibility of antioxidative enzymes in RGC-5 cells by IPRG001. In Figure 3A, 20 μM of IPRG001 significantly induced heme oxygenase-1 (HO-1) mRNA in RGC-5 cells 4-6 h after IPRG001 treatment (Figure 3A). Other antioxidative enzymes, such as NAD(P)H-quinone oxidoreductase-1 (NQO-1) and glutamate cystein ligase catalytic subunit (GCLC), were induced in RGC-5 cells 8-10 h after incubation of 20 μM IPRG001 (Figure 3A). A constitutive enzyme, heme oxygenase-2 (HO-2), was not increased by IPRG001 (Figure 3A). GAPDH mRNA did

not change during IPRG001 incubation. The levels of HO-1 mRNA and protein were quantified in Figure 3B (mRNA) and Figure 3C (protein). HO-1 mRNA and protein increased 1.6-1.8 fold in 4-6 h, then declined by 10 h after treatment. This time period of 4-6 h following treatment with IPRG001 in HO-1 induction was comparable to the pretreatment times of IPRG001 against H_2O_2 exposure (Figure 2B).

HO-1 induction in RGC-5 cells by IPRG001 and related drugs. ←----Fig. 4

To further confirm the correlation between HO-1 induction and NO generation by IPRG001, we investigated the effects of NO donor and NO scavenger on HO-1 induction by IPRG001. IPRG001 at 10-20 μM dose-dependently induced HO-1 mRNA expression (Figure 4A). 20 μM of IPRG001 increased HO-1 mRNA 1.8-fold 4 h following treatment (Figure 4A). This increase of HO-1 mRNA was blocked by c-PTIO (100 μM, Figure 4B). NOR1 at 50 μM increased HO-1 mRNA level 1.8-fold, compared to no treatment and this increase was also blocked by 100 μM of c-PTIO (Figure 4C).

HO-1 dependency of the neuroprotective action of IPRG001 in RGC-5 cells under H_2O_2 exposure. ←----Fig. 5

IPRG001 substantially induced antioxidative protein expression such as HO-1. It is very important to elucidate whether this HO-1 induction by IPRG001 is an effector molecule for its neuroprotection. In the presence of HO-1 specific inhibitor, SnMP (10 μM), the viability of RGC-5 cells with IPRG001 against H_2O_2 decreased from 80% to 60% in the absence of treatment (Figure 5A). SnMP alone did not change the cell viability in RGC-5 cells with or without H_2O_2 (Figure 5A). The neuroprotective action of NOR1 (50 μM) was also blocked by a combination of SnMP and NOR1 (data not

shown). Next, we examined the effects of siRNA specific to HO-1 mRNA. HO-1 mRNA levels were significantly reduced by siRNA treatment, but not by scrambled siRNA treatment (Figure 5B). The neuroprotective action of IPRG001 was also reduced by siRNA treatment, but not scrambled siRNA treatment. siRNA alone did not affect cell viability (Figure 5C).

IPRG001 induces release and translocation of Nrf2 to the nucleus in RGC-5 cells.

←----Fig. 6

To test the involvement of Nrf2 in the process of antioxidative HO-1 induction by IPRG001, we compared localization of Nrf2 in RGC-5 cells under 3 incubation conditions, (1) no treatment (Figures 6A-C), (2) 20 μM of IPRG001 (Figures 6D-F) and (3) IPRG001 plus c-PTIO (Figures 6G-I) in immunohistochemistry. Panels A, D and G show Nrf2 immunohistochemical staining images. Panels B, E and H show DAPI staining images. Panels C, F and I show merge images. When no treatment was given to RGC-5 cells, Nrf2 staining was diffusely in the cytoplasm (Figure 6A). IPRG001 induced intensive staining of Nrf2 in the nucleus (Figure 6D). This increase of nuclear staining of Nrf2 protein by IPRG001 was completely blocked with 100 μM of c-PTIO treatment (Figure 6G). c-PTIO alone did not affect any changes compared to no treatment (data not shown). Subcellular fractionation analysis further confirmed translocation of Nrf2 from cytoplasm to nucleus quantitatively. The levels of Nrf2 protein in the cytoplasm rapidly decreased 2-4 h following IPRG001 treatment, and then returned to the pre-stimulus levels by 6-8 h (Figure 6J). In contrast, the levels of Nrf2 protein in the nucleus rapidly increased 2-4 h following IPRG001 treatment, and gradually returned to the pre-stimulus condition 6-8 h (Figure 6K).

PI3K regulates IPRG001-induced Nrf2 accumulation to the nuclei in RGC-5 cells **←---- Fig. 7**

The mechanism of IPRG001-mediated Nrf2 translocation to the nuclei was explored. Immunostaining study showed translocation of Nrf2 by IPRG001 treatment for 2 h in RGC-5 cells (Figure 7). Although Nrf2 had diffusely localized cytoplasm under no treatment (Figure 7A-C), Nrf2 was translocated into DAPI-labeled nuclei by IPRG001 treatment (Figure 7D-F). Wortmannin (WT), a PI3K inhibitor, significantly inhibited nuclear translocation of Nrf2 (Figure 7 G-I). The proportion of Nrf2 translocation to the nuclei was calculated and graphed in Figure 7J. Both WT and LY294002 (LY), another PI3K inhibitor, significantly suppressed HO-1 induction by IPRG001 (Figure 7K). WT and LY alone did not affect HO-1 mRNA levels, when compared to no treatment. Next, we verify the importance of PI3K for cell survival associated with HO-1 expression by IPRG001. WT alone did not affect the cell viability of no treatment cells (Figure 7L). WT treatment 1 h before IPRG001 addition significantly decreased the cell survival of IPRG001 against H_2O_2 –induced cell death.

IPRG001 stimulates HO-1 expression through Nrf2/ARE pathway via S-nitrosylation of Keap1 **←---- Fig. 8**

To further assess the involvement of Nrf2 on HO-1 gene expression, we determined binding of Nrf2 to HO-1 enhancer E1 in the element of genomic HO-1 DNA. ChIP assays with an antibody directed against Nrf2 showed high binding of Nrf2 to the E1 enhancer. IPRG001 treatment for 2 h significantly enhanced Nrf2 binding to the E1 enhancer by about 3-fold (Figure 8A). 1 h pretreatment with c-PTIO before IPRG001 addition completely reversed increase in the binding of Nrf2 to E1 enhancer. The ChIP

assay with IgG did not show increased binding of Nrf2 to E1 enhancer, compared with no treatment (Figure 8A). Next, we investigated whether IPRG001 modified sensor molecule, intracellular Keap1 in the oxidative condition. After separation of free thiols and nitrosothiols of Keap1 protein, biotinylated nitrosothiols (S-nitrosylation) of Keap1 were isolated by avidin-coupled beads, and then measured by western blotting with anti-Keap1 antibody. S-nitrosylated proteins were increased 2-fold by IPRG001 compared to no treatment (Figure 8B). NOR1 also S-nitrosylated Keap1 3-fold. The increase of S-nitrosylation of Keap1 by IPRG001 was completely blocked by pretreatment with c-PTIO (Figure 8B). On the other hand, IPRG001 did not modify S-nitrosylation of caspase-3 (data not shown).

Neuroprotective action of IPRG001 in rat RGCs *in vivo* following nerve injury.

←---- Fig. 9

To further validate the protective effect of IPRG001 in rat RGCs *in vivo* after ONI, we first investigated induction of HO-1 expression in rat RGCs after intraocular injection of IPRG001 for 1 d. Figure 9A-F show HO-1 immunohistochemistry in rat retina. Panels (A-C) show the untreated retina (Figures 9A-C). Panels D-F show retina treated with IPRG001 (Figures 9D-F). Immunoreactivity of HO-1 was increased in the rat ganglion cell layer (GCL) by 0.1 nmol of IPRG001 (Figure 9D), compared to untreated retina (Figure 9A). The increase in HO-1 expression in GCL was confirmed to be localized in the RGC with TUJ-1 immunohistochemistry (Figure 9E). It could clearly be seen in the merged image (Fig. 9F).

Figures 9 G-L show TUNEL staining in the rat retina. Optic nerve crush induced apoptotic cell death of RGCs with TUNEL staining 7 d after injury (Figure 9I)

compared to the intact retina (Figure 9G). RGCs cell death after ONI was clearly blocked by pretreatment with 0.1 nmol IPRG001 (Figure 9K). This neuroprotective effect of IPRG001 in rat RGCs following nerve crush could not be seen by the original genipin (0.1 nmol/eye, Figure 9J), or IPRG001 (0.1 nmol/eye) plus SnMP (Figure 9L). SnMP alone did not affect RGC cell death (Figure 9H). Figure 9M illustrates the quantitative data of RGCs cell death after ONI. Finally we checked the appropriation of our rat ONI experiment as *in vivo* model of oxidative stress. We measured 4-hydroxynoneral (4HNE), a final product of lipid peroxidation (Koriyama *et al*., 2009b). Optic nerve crush increased 4HNE accumulation in the rat retina 1.4-fold at post lesioned 4 days compared to the intact retina (Figure 9N). Intraocular IPRG001 (0.1 nmol) significantly decreased the levels of ONI-induced 4HNE accumulation. The decreasing action of IPRG001 on 4HNE accumulation after nerve injury was significantly suppressed by co-injection of SnMP (Figure 9N). IPRG001 or SnMP alone did not change 4HNE accumulation.

Discussion

IPRG001 generates NO and induces HO-1 expression

The object of this study was to investigate the neuroprotective mechanism of genipin in neuronal cell line against oxidative stress conditions which we described previously (Yamazaki *et al*. 1996). The second purpose was to investigate the adaptability of the neuroprotective action of genipin to the nervous tissues *in vivo*. According to our previous NO-activating hypothesis for the neuritogenic action of genipin (Yamazaki *et al*. 2004), we examined a possible mechanism for genipin to exert neuroprotective action, through induction of antioxidative protein by NO activation. In the present study, we designed *in vitro* and *in vivo* models using rat retinal ganglion cells (RGC-5 cells and RGCs) against H_2O_2 exposure and ONI, respectively (Koriyama et al., 2008, 2009b). Under consideration of the structural lability of genipin (Fig. 9M), we used IPRG001, a long-acting alkyloxygenipin (Suzuki *et al*. 2010) throughout this study. Therefore, we first measured NO production by IPRG001 using NO sensitive fluorescent dye, DAF-2DA. Fluorescence was rapidly increased in RGC-5 cells within 0.5-4 h following IPRG001 exposure (Figure 1). We reported that genipin directly bound to neuronal nitric oxide synthase (nNOS) and thus activated nNOS to generate NO gas (Ohkubo *et al*. 2004, Suzuki *et al*., 2007). The binding of genipin to nNOS was based on its binding domain similar to that of tetrahydrobiopterin, a co-factor of nNOS (Suzuki *et al*. 2010). The neuroprotective action of IPRG001 was certainly NO dependent. NOR1, a NO donor, can be replaced by IPRG001 and c-PTIO, a NO scavenger clearly blocked the protective action of IPRG001 (Figure 2). The protective action of IPRG001 was completely blocked by CHX (Figure 2D). It strongly suggests that neuroprotection of IPRG001 is mediated by newly synthesizing protein(s). We showed that IPRG001 induced antioxidative enzymes, such as HO-1, NQO and GCLC

(Figure 3A). HO-1 (Maines, 1988, Poss and Tonegawa, 1997) is an enzyme, which degrades intracellular heme to free iron, carbon monoxide (CO) and biliverdin. CO plays a significant role in anti-apoptosis and anti-inflammation (Otterbein *et al*., 2000, 2003). Furthermore, bilirubin, converted from biliverdin (Nishimura *et al*., 1996) acts as reactive oxygen species scavenger and attenuates lipid peroxidation related 4HNE (Deguchi *et al*., 2008). Biliverdin also exerts anti-inflammatory and neuroprotective effects (Hung *et al*., 2010). In this study, induction of HO-1 by IPRG001 in RGC-5 cells was also NO dependent (Figure 4). SnMP and HO-1 siRNA showed the partial cancellation of IPRG001 protection against oxidative stress. HO-1 mainly involves in the survival effect against oxidative stress. However we can not deny that NQO-1 and/or GCLC have the neuroprotective effect because they are also induced within 24 h. The data all together strongly indicate that the neuroprotective action of IPRG001 is caused by NO generation following antioxidant HO-1 induction in RGC-5 cells against H_2O_2. Furthermore, the crucial role HO-1 plays as an effector molecule for the neuroprotection by IPRG001 was confirmed by specific HO-1 inhibitor, SnMP and siRNA specific to HO-1 (Figure 5).

IPRG001 S-nitrosylates Keap1 and activates Nrf2/ARE pathway in RGC-5 cells against oxidative stress.

IPRG001 induced antioxidative enzymes, such as HO-1, NQO and GCLC, in RGC-5 cells (Figure 3A). Especially, HO-1 was expressed in a NO-dependent manner (Figure 4). Thus, we next investigated the signaling pathway leading to induction of these proteins. It is well known that such antioxidative enzymes are induced by various electrophilic compounds, including the oxygen radicals (Wakabayashi *et al*., 2004, Hong *et al*., 2005). Therefore, we tested the possibility to induce HO-1 through the

Nrf2/ARE pathway under NO stimulus condition generated by IPRG001. It is well known that Nrf2 is a key transcriptional factor for the induction of antioxidative enzymes against oxidative stress (Kaspar *et al*., 2009). IPRG001 rapidly induced release and nuclear translocation of Nrf2 within 2-4 h, and then the levels of Nrf2 in nucleus were returned to the pre-stimulus condition 6-8 h after exposure (Figure 6). Translocation of Nrf2 was PI3K dependent, because wortmannin and LY 294002 completely blocked all these processes: translocation, neuroprotection and HO-1 induction by IPRG001. The release and translocation of Nrf2 being dependent upon PI3K was reported in various cell types (Nakaso *et al*., 2003, Martin *et al*., 2004). Although the ARE for HO-1 gene remains unclear, E1 enhancer was identified as a candidate of ARE for HO-1 gene (Alam and Cook 2003, Liu *et al*. 2007). In our data, the several antioxidative enzymes including HO-1, NQO-1 and GCLC were induced by addition of IPRG001 in a different time frame. One of the reasons may be in the difference of ARE site and/or its binding affinity of Nrf2 in each enzyme. Actually, E1 enhancer is known as a specific ARE to HO-1 and has different DNA sequences of ARE from that of the other enzymes'ARE (Alam and Cook, 2003). By using the ChIP method, we confirmed increased levels of Nrf2 bound to the E1 enhancer in RGC-5 cells treated with IPRG001 (Figure 8A). c-PTIO completely blocked binding of Nrf2 to the E1 element. The release and translocation of Nrf2 from the cytoplasm to the nucleus was initiated by modifications of intracellular sensor protein, Keap1. NO activated the Nrf2/ARE pathway by S-nitrosylation of Keap1 protein in colon carcinoma cells (Li *et al*., 2009). In this study, NO certainly S-nitrosylated Keap1 protein by biotin-switch assay (Figure 8B). IPRG001 and NOR1 S-nitrosylated Keap1 2-3-fold following exposure, compared to no treatment. c-PTIO clearly blocked this modifications. In this study, Keap1 is the molecule which can regulate Nrf2 translocation by its

S-nitrosylation of cysteine residues and threby promotes the transcription of antioxidative enzymes. Although we can not yet provide precise target of S-nitrosylation in Keap1 protein, two reactive cysteines, Cys273 and Cys288, of Keap1 have been identified as determinant site of translocational activity of Nrf2 at least (Buckley et al., 2008). Tomita *et al*. (2002) reported that the neuroprotective action of nipradilol in the PC12 cells against serum deprivation was due to inhibition of caspase-3 via S-nitrosylation. In this study, it was not the case of caspase-3 S-nitrosylation. These results demonstrate for the first time that the neuroprotective action of IPRG001 is caused by induction of HO-1 antioxidative protein in the neuronal cells (RGC-5 cells) through the Nrf2/ARE pathway from NO generation to Keap1 S-nitrosylation.

Neuroprotective action of IPRG001 in the rat RGCs in vivo after nerve injury.

In our previous publication (Homma *et al*. 2007), more than half of rat RGCs became apoptotic 6-7 days after ONI. The RGC cell death following nerve crush was partly caused by hydroxy radical or super oxide anion (Levkovitch-Verbin *et al*. 2000). Therefore, cell death was blocked by antioxidants (Castagné and Clarke 1996). In this study ONI increased 4HNE accumulation in the retina by 1.4-fold (Figure 9N). Therefore, we used rat RGCs after ONI as an *in vivo* model of oxidative stress. Intraocular injection of 0.1 nmol IPRG001 specifically induced HO-1 expression in the RGCs 1 d post-injection (Figure 9D). This RGCs localization was confirmed by a specific marker of RGCs (Figure 9E). IPRG001 also induced NADPH diaphorase activity (NO synthase activity) in the RGCs (Y. Koriyama unpublished data). These results suggest that IPRG001 induces HO-1 expression via NO generation. It is well known that HO-1 expression in the RGCs is induced as a self-defense system following ischemia/reperfusion insults (Peng *et al*., 2008). Further studies are needed to elucidate

the molecular signaling of this HO-1 induction in the retina *in vivo* by IPRG001.

RGC cell death after nerve crush was almost completely protected by IPRG001, as demonstrated by TUNEL staining (Figure 9K). This protection depended on the HO-1 induction, because the protective action of IPRG001 was suppressed by co-injection with HO-1 inhibitor, SnMP (Figures 9L and 9M). IPRG001 decreased the levels of 4HNE accumulation in the retina after ONI. The reducing action of IPRG001 on 4HNE accumulation was also significantly suppressed by SnMP (Figure 9N). The present results demonstrate for the first time that genipin protects rat RGC cell death *in vitro* and *in vivo* against oxidative stress by antioxidant HO-1 induction via the Nrf2/ARE pathway. The neurotrophic actions - neuritogenesis and neuroprotection - of genipin become a useful therapeutic tool to rescue degenerative neuronal diseases, such as glaucoma.

Acknowledgments

We thank Ms Sachiko Higashi and Tomoko Kano for their administrative and technical assistance. This work was partly supported by research grants from the Ministry of Education, Culture, Sports, Science and Technology of Japan (Nos 22791651 to YK, 22300109 to SK, 20254001 to KM), “Academic Frontier” Project for Private Universities (2005-2009), and Mitani Scientific Foundation (to YK).

References

Alam J. and Cook J. L. (2003) Transcriptional reguration of the heme oxygenase-1 gene via the stress response element pathway. Curr. Pharm. Des. 9: 2499–2511.

Buckley B. J., Li S., Whorton A. R. (2008) Keap1 modification and nuclear

accumulation in response to S-nitrosocysteine. Free Radic. Biol. Med. 44, 692-698.

Castagné V. and Clarke P. G. (1996) Axotomy-induced retinal ganglion cell death in development: its time-course and its diminution by antioxidants. Proc. Biol. Sci. 263, 1193-1197.

Deguchi K., Hayashi T., Nagotani S., Sehara Y., Zhang H., Tsuchiya A., Ohta Y., Tomiyama K., Morimoto N., Miyazaki M., Huh N. H., Nakao A., Kamiya T. and Abe K. (2008) Reduction of cerebral infarction in rats by biliverdin associated with amelioration of oxidative stress. Brain Res. 1188, 1-8.

Homma K., Koriyama Y., Mawatari K., Higuchi Y., Kosaka J. and Kato S. (2007) Early downregulation of IGF-I decides the fate of rat retinal ganglion cells after optic nerve injury. Neurochem. Int. 50, 741-748.

Hong F., Sekhar K. R , Freeman M. L., and Liebler D. C. (2005). Specific patterns of electrophile adduction trigger Keap1 ubiquitination and Nrf2 activation. J. Biol. Chem. 280, 31768-81775.

Hung S. Y., Liou H. C. and Fu W. M. (2010) The mechanism of heme oxygenase-1 action involved in the enhancement of neurotrophic factor expression. Neuropharmacol. 58, 321-329.

Jaffrey S. R., Erdjument-Bromage H., Ferris C. D., Tempst P. and Snyder S. H. (2001) Protein S-nitrosylation: a physiological signal for neuronal nitric oxide. Nat. Cell Biol. 3, 193-197.

Kaspar J. W., Niture S. K. and Jaiswal A.K. (2009) Nrf2:INrf2 (Keap1) signaling in oxidative stress. Free Rad. Biol. Med. 47, 1304-1309.

Koriyama Y., Chiba K., and Mohri T. (2003) Propentofylline protects β-amyloid protein-induced apoptosis in cultured rat hippocampal neurons. Eur. J. Pharmacol. 458, 235-241.

Koriyama Y., Tanii H., Ohno M., Kimura T. and Kato S. (2008) A novel neuroprotective role of a small peptide from flesh fly, 5-S-GAD in the rat retina in vivo. Brain Res. 1240, 196-203.

Koriyama Y., Yasuda R., Homma K., Mawatari K., Nagashima M., Sugitani K., Matsukawa T. and Kato S. (2009a) Nitric oxide-cGMP signaling regulates axonal elongation during optic nerve regeneration in the goldfish in vitro and in vivo. J. Neurochem. 110, 890-901.

Koriyama Y., Ohno M., Kimura T. and Kato S. (2009b) Neuroprotective effects of 5-S-GAD against oxidative stress-induced apoptosis in RGC-5 cell. Brain Res. 1296, 187-195.

Kurauchi Y., Hisatsune A., Isohama Y. and Katsuki H. (2009) Nitric oxide-cyclic GMP signaling pathway limits inflammatory degeneration of midbrain dopaminergic neurons: cell type-specific regulation of heme oxygenase-1 expression. Neuroscience. 158, 856-866.

Levkovitch-Verbin, H, Harris-Cerruti, C, Groner, Y, Wheeler, LA, Schwartz, M, and Yoles, E. (2000) RGC death in mice after optic nerve crush injury: oxidative stress and neuroprotection Invest. Ophthalmol. Vis. Sci. 41, 4169-4174

Li C. Q., Kim M. Y., Godoy L. C., Thiantanawat A., Trudel L. J. and Wogan G. N. (2009) Nitric oxide activation of Keap1/Nrf2 signaling in human colon carcinoma cells. Proc. Natl. Acad. Sci. USA. 106, 14547-14551.

Liu X. M., Peyton K. J., Ensenat D., Wang H., Hannink M., Alam J., and Durante W. (2007) Nitric oxide stimulates heme oxygenase-1 gene transcription via the Nrf2/ARE complex to promote vascular smooth muscle cell survival. Cardiovasc. Res. 75, 381-389.

Maines M. D. (1988) Heme oxygenase: function, multiplicity, regulatory mechanisms,

and clinical applications. FASEB J. 2, 2557-2568.

Martin D., Rojo A. I., Salinas M., Diaz R., Gallardo G., Alam J., De Galarreta C. M., and Cuadrado A . (2004) Regulation of heme oxygenase-1 expression through the phosphatidylinositol 3-kinase/Akt pathway and the Nrf2 transcription factor in response to the antioxidant phytochemical carnosol. J. Biol. Chem. 279, 8919-8929.

Nakaso K., Yano H., Fukuhara Y., Takeshima T., Wada-Isoe K. and Nakashima K. (2003) PI3K is a key molecule in the Nrf2-mediated regulation of antioxidative proteins by hemin in human neuroblastoma cells. FEBS Lett. 546, 181-184.

Nishimura R. N., Dwyer B. E. and Lu S. Y. (1996) Localization of heme oxygenase in rat retina: effect of light adaptation. Neurosci. Lett. 205, 13-16.

Ohkubo T., Yamazaki M., Yoshida A., Chiba K., and Mohri T. (2004) Detection of genipin/geniposide-target molecules by a geniposide overlay method using anti-geniposide antibody. J. Health Sci., 50, 193-196.

Otterbein L. E., Bach F. H., Alam J., Soares M., Tao Lu H., Wysk M., Davis R. J, Flavell R. A. and Choi A. M. (2000) Carbon monoxide has anti-inflammatory effects involving the mitogen-activated protein kinase pathway. Nat. Med. 6, 422-428.

Otterbein L. E, Zuckerbraun B. S., Haga M., Liu F., Song R., Usheva A., Stachulak C., Bodyak N., Smith R. N., Csizmadia E., Tyagi S., Akamatsu Y., Flavell R. J., Billiar T. R.,Tzeng E., Bach F. H., Choi A.M. and Soares M. P. (2003) Carbon monoxide suppresses arteriosclerotic lesions associated with chronic graft rejection and with balloon injury. Nat. Med. 9, 183-190.

Peng P. H., Ko M. L., Chen C. F. and Juan S. H. (2008) Haem oxygenase-1 gene transfer protects retinal ganglion cells from ischaemia/reperfusion injury. Clin. Sci. 115, 335-342.

Poss K. D. and Tonegawa S. (1997) Reduced stress defense in heme oxygenase

1-deficient cells. Proc. Natl. Acad. Sci. U S A. 94, 10925-10930.

Suzuki H., Yamazaki M., Chiba K., Sawanishi H. (2007) Characteristic properties of genipin as an activator in neuronal nitric oxide synthase. J. Health Sci., 53, 730-733.

Suzuki H., Yamazaki M., Chiba K., Uemori Y. and Sawanishi H. (2010) Neuritogenic activities of 1-alkyloxygenipins. Chem. Pharm. Bull. 58, 168-171.

Tomita H., Nakazawa T., Sugano E., Abe T. and Tamai M. (2002) Nipradilol inhibits apoptosis by preventing the activation of caspase-3 via S-nitrosylation and the cGMP-dependent pathway. Eur. J. Pharmacol. 452, 263-268.

Wakabayashi N., Dinkova-Kostova A. T., Holtzclaw W. D., Kang M. I., Kobayashi A., Yamamoto M., Kensler T. W., and Talalay P. (2004) Protection against electrophile and oxidant stress by induction of the antioxidant enzymes response: fate of cysteines of the Keap1 sensor modified by inducers. Proc. Natl. Acad. Sci. U. S. A. 101, 2040-2045.

Yamazaki M., Chiba K. and Mohri T. (1996) Neuritogenic effect of natural iridoid compounds on PC12h cells and its possible relation to signaling protein kinases. Biol. Pharm. Bull. 19, 791-795.

Yamazaki M., Chiba K., Mohri T. and Hatanaka H. (2001a) Activation of the mitogen-activated protein kinase cascade through nitric oxide synthesis as a mechanism of neuritogenic effect of genipin in PC12h cells. J. Neurochem. 79, 45-54.

Yamazaki M., Sakura N., Chiba K. and Mohri T. (2001b) Prevention of the neurotoxicity of the amyloid beta protein by genipin. Biol. Pharm. Bull. 24, 1454-1455.

Yamazaki M., Chiba K., Mohri T. and Hatanaka H. (2004) Cyclic GMP-dependent neurite outgrowth by genipin and nerve growth factor in PC12h cells. Eur. J. Pharmacol. 488, 35-43.

Yamazaki M. and Chiba K. (2005) Neurotrophic Effects of Genipin on Neuro2a Cells. J. of Health Sci. 51, 687-692.

Yamazaki M., Chiba K. and Satoh K. (2008) Neuro2a Cell Death Induced by 6-Hydroxydopamine is Attenuated by Genipin. J. Health Sci. 54, 638-644.

Figure legends

Fig. 1

NO production by IPRG001 in RGC-5 cells. NO production levels by IPRG001 in RGC-5 cells were evaluated and observed by DAF-2DA staining (A, B, D). RGC-5 cell nuclei were stained with DAPI (C, E). (A) Quantitative data for fluorescence intensity were measured by fluorescence plate reader. *P<0.01 vs. 0 h (n=4). (B, C) No treated cells. (D, E) Treated cells with 20 μM IPRG001 for 1 h. Scale = 20 μm.

Fig. 2

Protective effect of IPRG001 on cell death of RGC-5 cells induced by H_2O_2 exposure. Cell viability was estimated by MTT assay. (A) Cell viability of RGC-5 cells was performed with IPRG001 at various concentrations 4 h prior to 300 μM H_2O_2 exposure for 24 h. (B) Various pretreatment times of IPRG001 to 300 μM H_2O_2 exposure. The pretreatment of 4-6 h with IPRG001 was sufficient to prevent from H_2O_2-induced cell death. *P<0.01 vs. no treatment (n=6). (C) RGC-5 cells were pretreated with NOR1 at various concentrations for 4 h and then cultured with 300 μM H_2O_2 for 24 h. (D) A NO-scavenger, c-PTIO or an inhibitor of protein synthesis, cycloheximide (CHX) was first treated 1 h prior to IPRG001 addition, and then IPRG001 was added 4 h prior to the H_2O_2 and finally H_2O_2 was added to RGC-5 cells for further 24 h. *P<0.01 vs. no treatment; +P<0.01 vs. H_2O_2 alone (n=6).

Fig. 3

Induction of antioxidative enzymes in RGC-5 cells by IPRG001. (A) Candidate antioxidant genes upregulated after IPRG001 treatment in RGC-5 cells. (B) Upregulation of HO-1 mRNA in RGC-5 cells after IPRG001 treatment. *P<0.01 vs. 0 h (n=3). (C) Upregulation of HO-1 protein after IPRG001 treatment. *P<0.01 vs. 0 h (n=3).

Fig. 4

HO-1 induction by IPRG001 through NO dependent mechanism. (A) IPRG001 induced HO-1 mRNA expression in dose-dependent manner after 4 h treatment *P<0.01 vs. 0 μM (n=3). (B) c-PTIO cancelled the HO-1 mRNA induction by IPRG001 *P<0.01 vs. no treatment (n=3). (C) c-PTIO cancelled the HO-1 mRNA induction by NOR1 *P<0.01 vs. no treatment (n=3).

Fig. 5

HO-1 dependent protection of IPRG001 in RGC-5 cells. (A) A HO-1 inhibitor, SnMP cancelled the neuroprotection by IPRG001 against H_2O_2 *P<0.01 vs. no treatment (n=6). (B) Decreased levels of HO-1 mRNA following treatment with HO-1 specific siRNA relative to the no treatment or scrambled siRNA. *P<0.01 vs. no treatment (n=3). (C) HO-1 specific siRNA significantly cancelled neuroprotective action by IPRG001 against H_2O_2 *P<0.01 vs. no treatment (n=6).

Fig. 6

Translocation of Nrf2 to nucleus by IPRG001. (A, D, G,) Immunohistochemical staining of Nrf2. C-PTIO was treated 1 h prior to IPRG001 addition. (A) No treatment, (D) IPRG001 at 20 μM for 2 h, (G) IPRG001 with c-PTIO. (B, E, H) DAPI staining, (C,

F, I) Merged images. Scale bar= 10 μm. (J) Levels of Nrf2 protein in cytoplasm fractions treated with IPRG001 at various exposure times. *P<0.01 vs. 0 h (n=3). (K) Levels of Nrf2 protein in nuclear fractions treated with IPRG001 at various exposure times. *P<0.01 vs. 0 h (n=3).

Fig. 7

PI3K regulates the IPRG001-induced Nrf2 accumulation to nuclei in RGC-5 cells. (A, D, G) Immunohistochemical study on Nrf2. (A) No treatment, (D) IPRG001 treatment for 2 h, (G) Wortmannin (WT) pretreatment for 1 h before IPRG001 addition. (B, E, H) DAPI staining. (C, F, I) Merged images. Scale bar = 20 μm. (J) Evaluation of Nrf2 translocation to nuclei. We counted the number of Nrf2 stained cells per total DAPI-stained cells. *P<0.01 vs. no treatment (n=30); +P<0.01 vs. IPRG001 alone (n=30). (K) PI3K dependent HO-1 induction by IPRG001. PI3K inhibitors, wortmannin (WT) or LY294002 (LY) completely suppressed the levels of HO-1 mRNA expression induced by IPRG001. *P<0.01 vs. no treatment (n=3). (L) PI3K regulates neuroprotection by IPRG001. WT completely cancelled neuroprotective effect of IPRG001 against H_2O_2 –induced cell damages. *P<0.01 vs. no treatment; +P<0.01 vs. H_2O_2 alone (n=6).

Fig. 8

IPRG001 stimulates Nrf2 binding to the HO-1 promoter and S-nitrosylation of Keap1. (A) ChIP assay demonstrates binding of Nrf2 to the HO-1 E1 enhancer following treatment of IPRG001 for 2 h with or without c-PTIO pretreatment for 1 h. The band shows PCR products of E1 enhancer. (B) S-Nitrosylation of Keap1 by IPRG001. RGC-5 cells were exposed to 20 μM IPRG001 for 1 h and submitted to biotin-switch

assay of protein. Biotinylated proteins were mixed with avidin-beads eluted and analyzed by Western blotting with anti-Keap1 antibody. *P<0.01 vs. no treatment (n=3).

Fig. 9

HO-1 induction and neuroprotective effect of IPRG001 in the rat retina *in vivo*. (A-F) HO-1 induction by IPRG001 in the rat retina. (A, D) No treated retina (A) and intraocularly injected retina with IPRG001 for 1 day (D). (B, E) TUJ-1-positive RGCs in no treatment (B) and IPRG001 treated retina (E). (C, F) Merged images. (G-L) TUNEL staining in retina after optic nerve injury for 7 days. (G) Intact retina, (H) SnMP at 0.1 nmol, (I) optic nerve injured retina, (J) genipin at 0.1 nmol (K) injury plus IPRG001, (L) injury plus IPRG001 with SnMP. Scale bar = 100 μm. (M) Graphical representation of number of TUNEL-positive cells in the GCL in visual fields. *P< 0.01 vs. intact retina, +P<0.01 vs. injury (n=30). (N) Prevention of nerve injury induced 4HNE production by IPRG001 via HO-1 activation. 4HNE production was measured by dot blotting analyses with an anti-4HNE antibody. Graphical representation of 4HNE bands in the blot. *P< 0.01 vs. intact retina, +P<0.01 vs. injury, #P<0.01 vs injury plus IPRG001. (n=3).

Fig.1

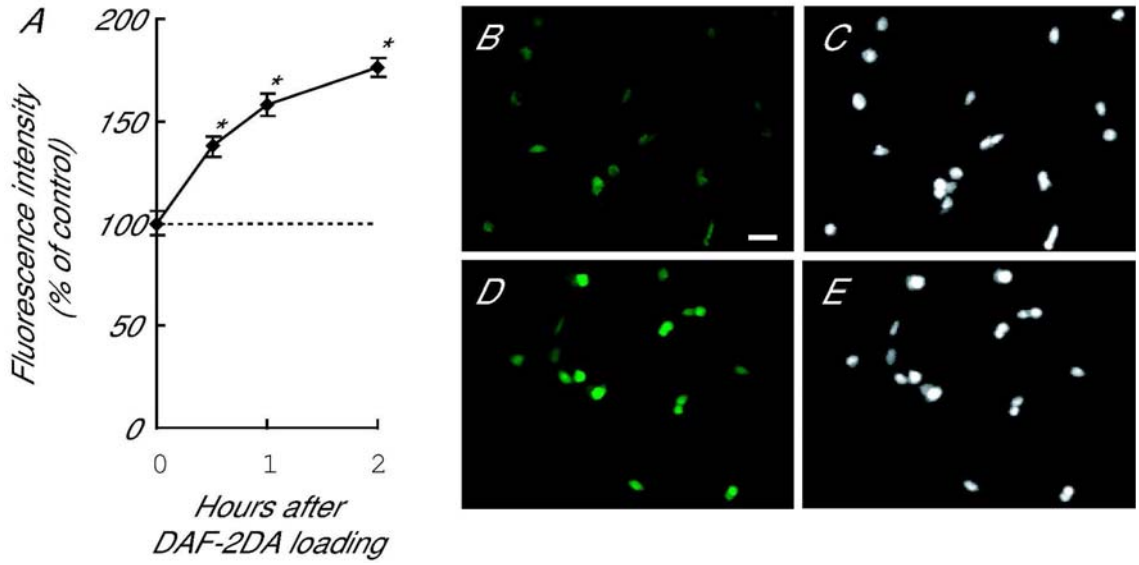

Fig.2

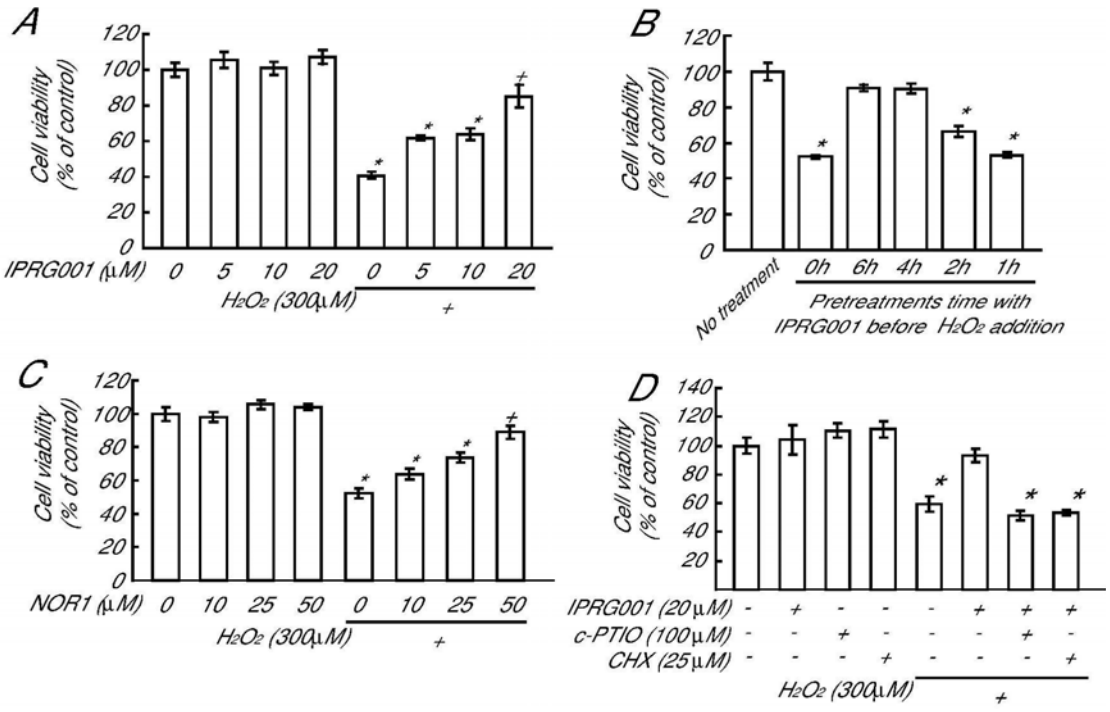

Fig.3

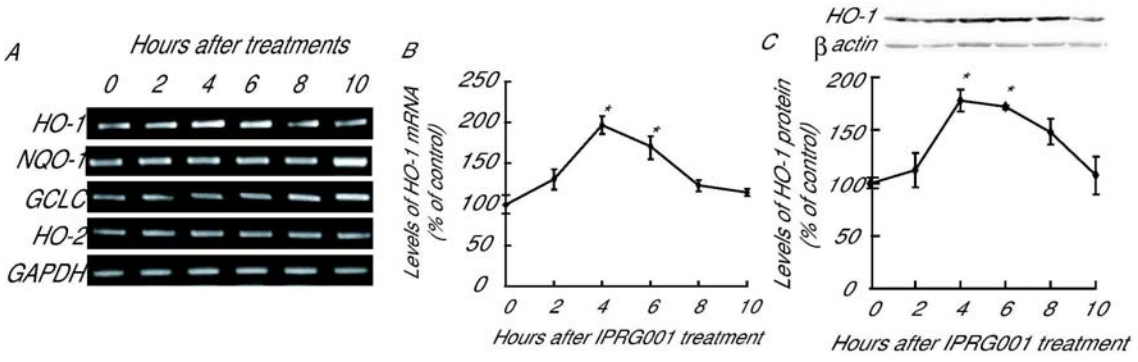
A
Hours after treatments
0 2 4 6 8 10
HO-1
NQO-1
GCLC
HO-2
GAPDH
B
Levels of HO-1 mRNA (% of control)
250
200
150
100
50
0
0 2 4 6 8 10
Hours after IPRG001 treatment
C
HO-1
β actin
Levels of HO-1 protein (% of control)
200
150
100
50
0
0 2 4 6 8 10
Hours after IPRG001 treatment

Fig.4

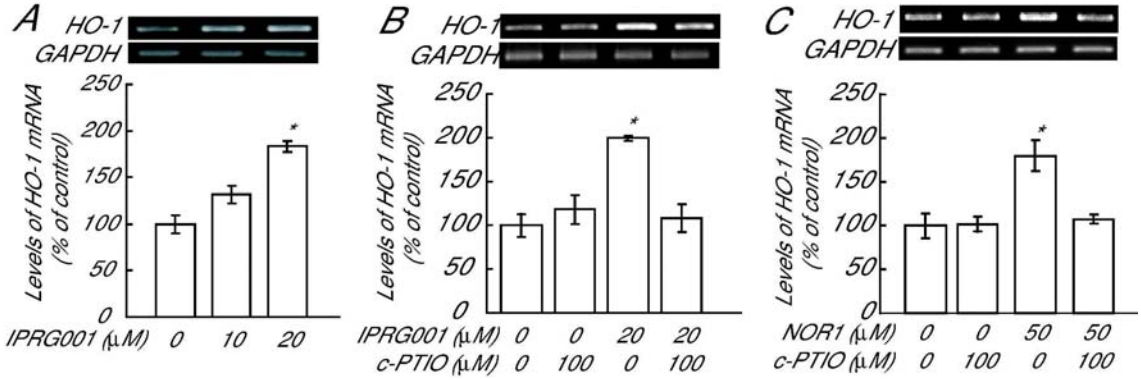
A
HO-1
GAPDH
Levels of HO-1 mRNA (% of control)
250
200
150
100
50
0
IPRG001 (μM) 0 10 20
B
HO-1
GAPDH
Levels of HO-1 mRNA (% of control)
250
200
150
100
50
0
IPRG001 (μM) 0 0 20 20
c-PTIO (μM) 0 100 0 100
C
HO-1
GAPDH
Levels of HO-1 mRNA (% of control)
250
200
150
100
50
0
NOR1 (μM) 0 0 50 50
c-PTIO (μM) 0 100 0 100

Fig.5

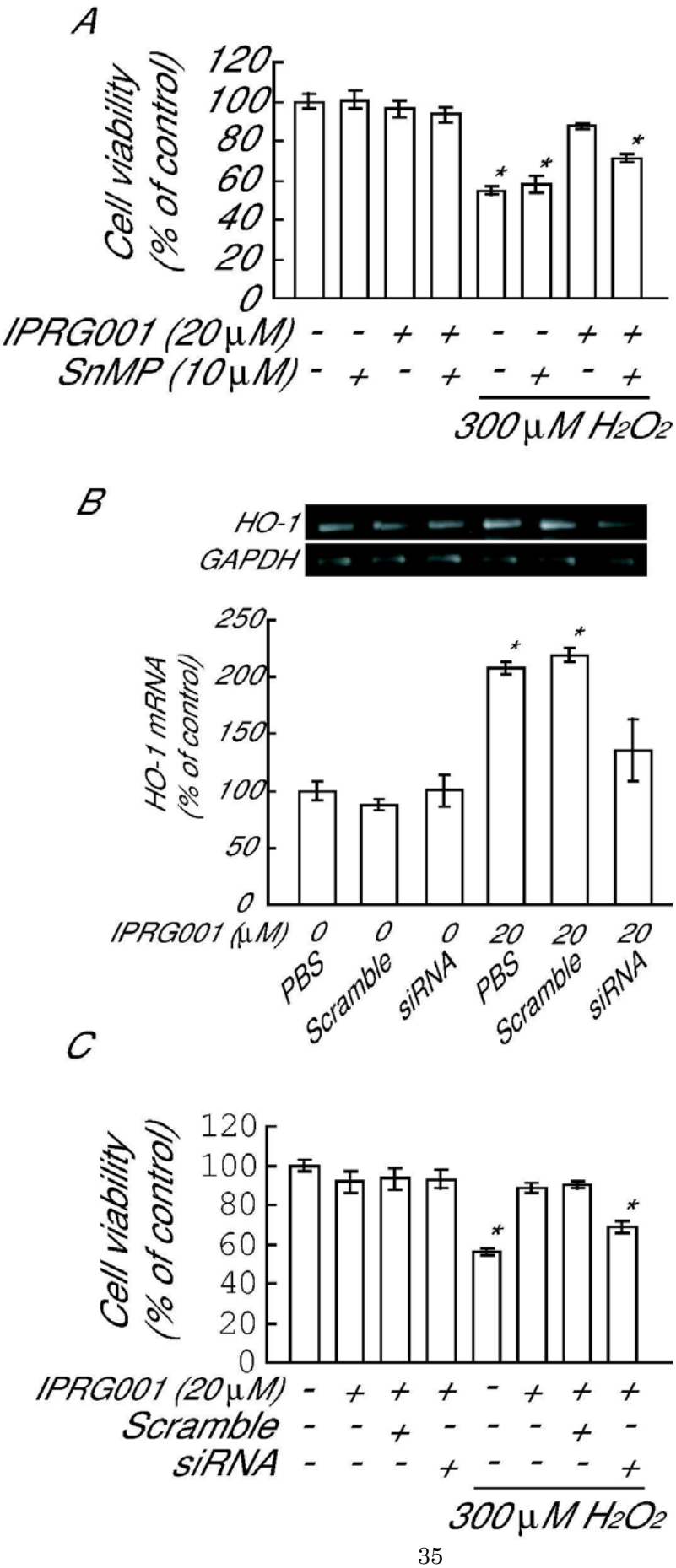
A
Cell viability (% of control)
120
100
80
60
40
20
0
IPRG001 (20μM) - - + + - - + +
SnMP (10μM) - + - + - + - +
300μM H2O2
B
HO-1
GAPDH
HO-1 mRNA (% of control)
250
200
150
100
50
0
IPRG001 (μM) 0 0 0 20 20 20
PBS
Scramble
siRNA
PBS
Scramble
siRNA
C
Cell viability (% of control)
120
100
80
60
40
20
0
IPRG001 (20μM) - + + + - + + +
Scramble - - + - - - + -
siRNA - - - + - - - +
300μM H2O2

Fig.6

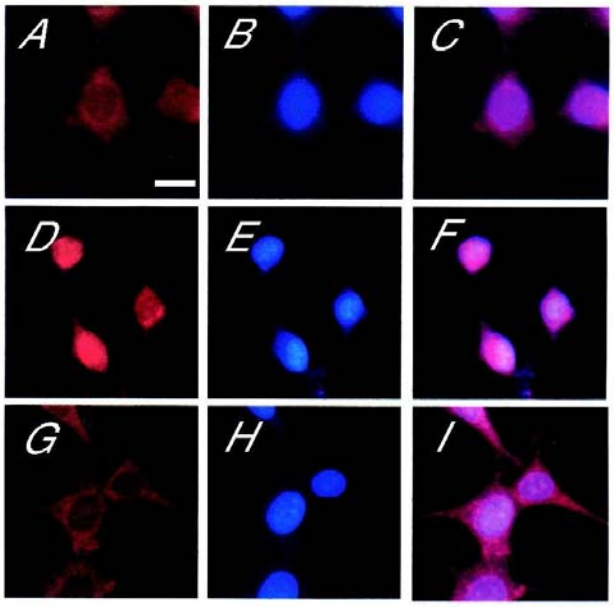
A
B
C
D
E
F
G
H
I

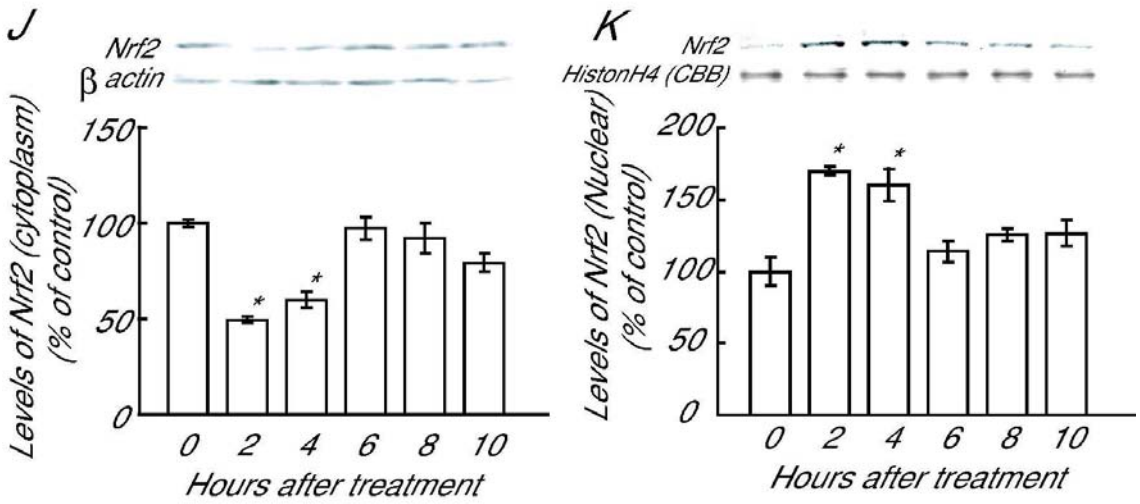
J
Nrf2
β actin
Levels of Nrf2 (cytoplasm) (% of control)
150
100
50
0
0 2 4 6 8 10
Hours after treatment
K
Nrf2
HistonH4 (CBB)
Levels of Nrf2 (Nuclear) (% of control)
200
150
100
50
0
0 2 4 6 8 10
Hours after treatment

Fig.7

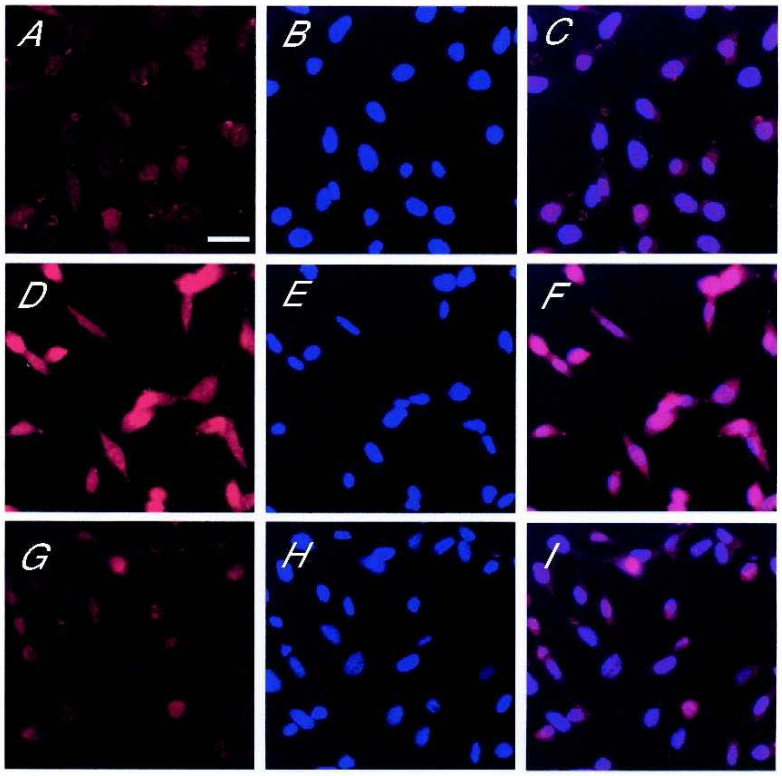
A
B
C
D
E
F
G
H
I

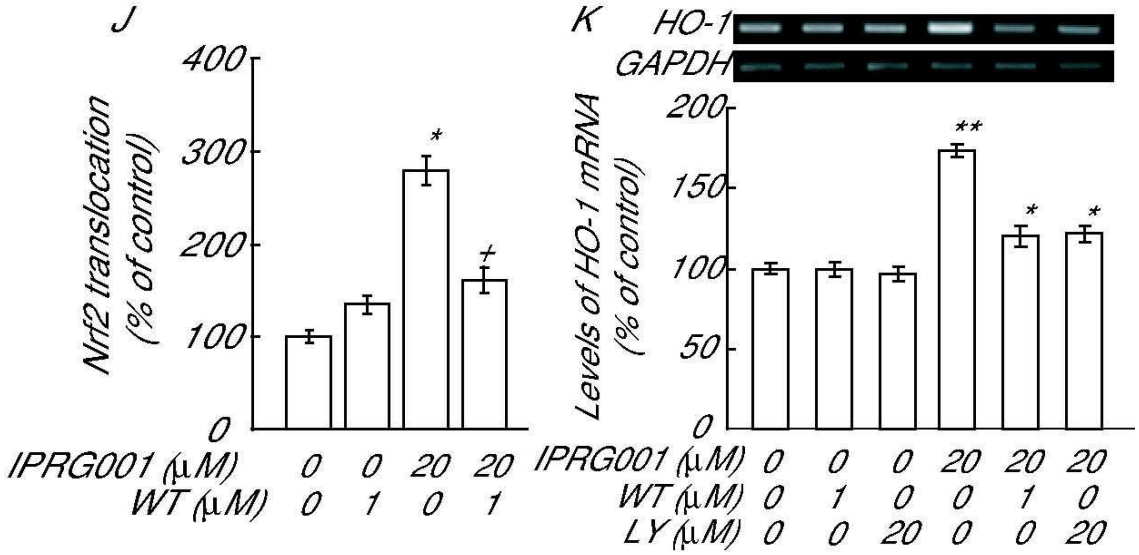
J
Nrf2 translocation (% of control)
400
300
200
100
0
*
≠
IPRG001 (μM) 0 0 20 20
WT (μM) 0 1 0 1
K
HO-1
GAPDH
Levels of HO-1 mRNA (% of control)
200
150
100
50
0
**
*
*
IPRG001 (μM) 0 0 0 20 20 20
WT (μM) 0 1 0 0 1 0
LY (μM) 0 0 20 0 0 20

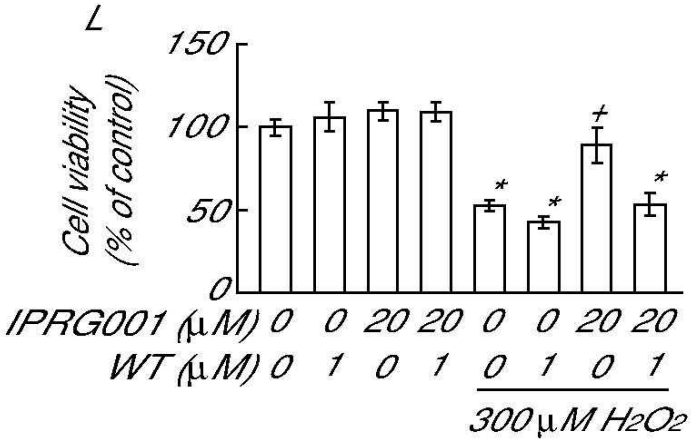
L
Cell viability (% of control)
150
100
50
0
*
*
≠
*
IPRG001 (μM) 0 0 20 20 0 0 20 20
WT (μM) 0 1 0 1 0 1 0 1
300 μM H2O2

Fig.8

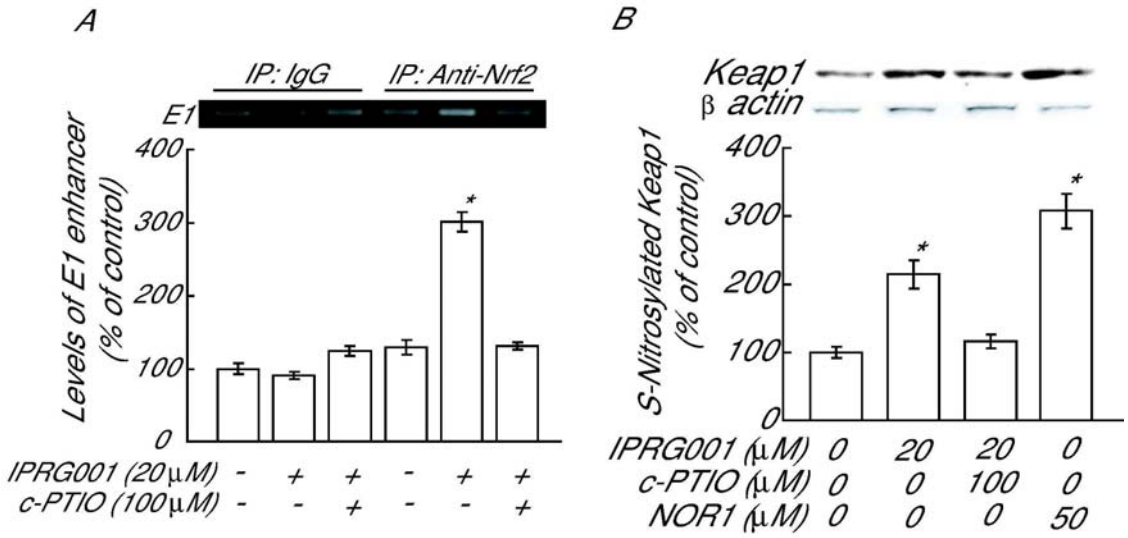
A
IP: IgG
IP: Anti-Nrf2
E1
Levels of E1 enhancer (% of control)
400
300
200
100
0
*
IPRG001 (20μM) - + + - + +
c-PTIO (100μM) - - + - - +
B
Keap1
β actin
S-Nitrosylated Keap1 (% of control)
400
300
200
100
0
*
*
IPRG001 (μM) 0 20 20 0
c-PTIO (μM) 0 0 100 0
NOR1 (μM) 0 0 0 50

Fig.9

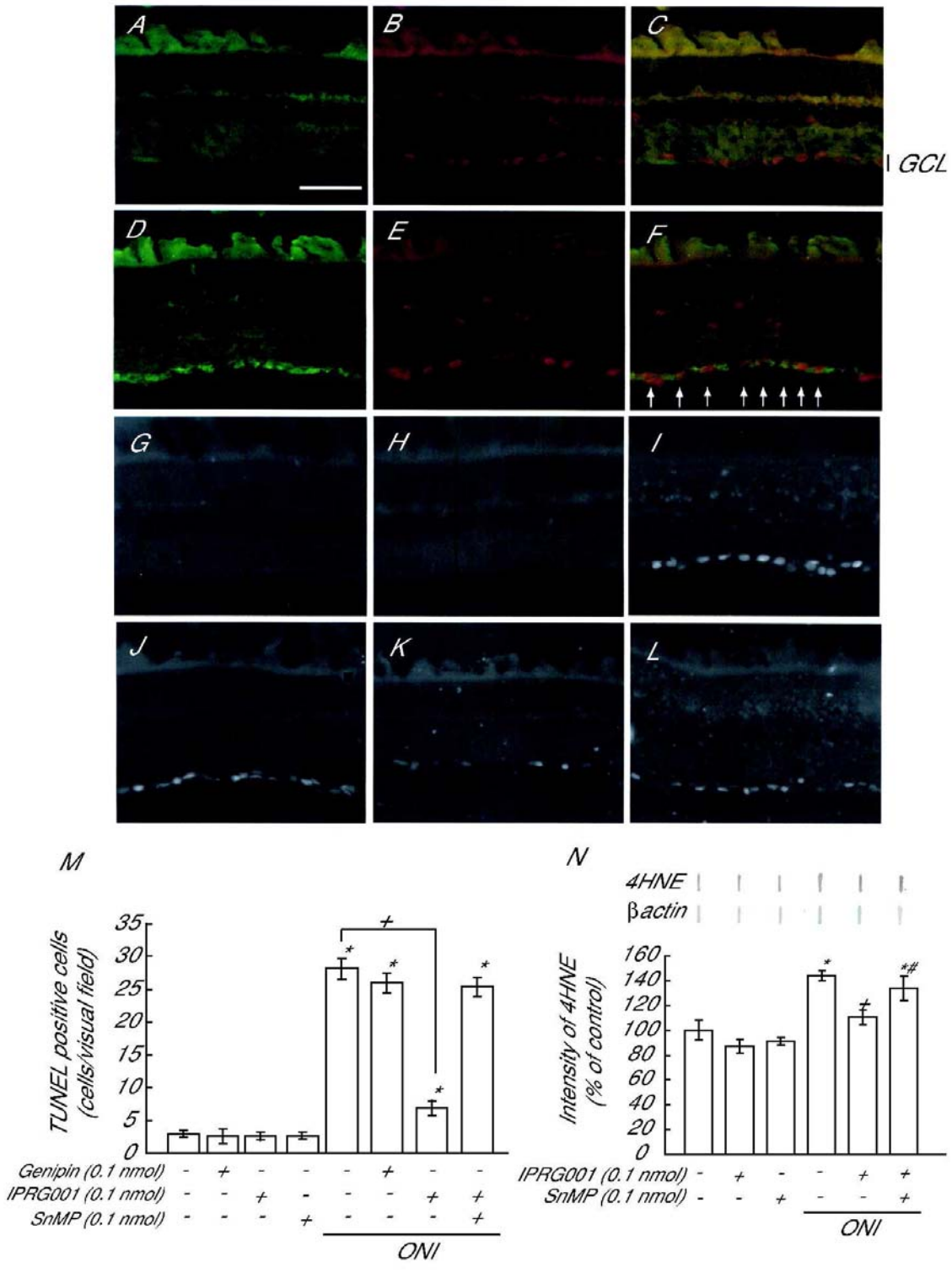
A
B
C
GCL
D
E
F
G
H
I
J
K
L
M
TUNEL positive cells
(cells/visual field)
35
30
25
20
15
10
5
0
Genipin (0.1 nmol)
IPRG001 (0.1 nmol)
SnMP (0.1 nmol)
ONI
N
4HNE
βactin
Intensity of 4HNE
(% of control)
160
140
120
100
80
60
40
20
0
IPRG001 (0.1 nmol)
SnMP (0.1 nmol)
ONI